# IMPACTS OF COAL MINING SUBSIDENCE ON LAND USE AND ECOLOGICAL SERVICES IN TAIBAI LAKE DISTRICT IN JINING CITY, CHINA

ZHENG, G. D.[1,2] – XIAO, N.[1,2] – LIU, K.[1,2] – XU, H. P.[1,2*] – BO, H. Z.[1,2]

[1]*Shandong Provincial Lunan Geology and Exploration Institute (Shandong Provincial Bureau of Geology and Mineral Resources No.2 Geological Brigade), Jining, China*

[2]*Technology Innovation Center of Restoration and Reclamation in Mining-induced Subsidence Land, Ministry of Natural Resources, Jining, China*

**Corresponding author*
*e-mail: xuhepeng2025@163.com; phone: +86-178-0537-5644*

(Received 9th May 2025; accepted 26th Jun 2025)

**Abstract.** As the primary energy source in China, the extensive mining of coal has led to the emergence of many coal resource-based cities. However, the phenomenon of coal mining subsidence has severely hindered urban development and adversely affected the ecosystem service values (ESV). This study employs an analysis of land use changes alongside a grey relational degree model to investigate the evolution of land use and the driving factors influencing ESV in the Taibai Lake District of Jining City, China, from 2000 to 2021. The findings reveal the following: (1) Farmland and water bodies were the predominant land use types. The area of farmland initially experienced a decline followed by an increase, while the area of water bodies exhibited the opposite trend. The primary land use transitions were farmland-to-water and farmland-to-construction land. Landscape fragmentation, uniformity, and diversity rose from 2000-2016 but declined afterwards, indicating pattern optimization. (2) Total ESV rose significantly until 2018, then slightly decreased in 2021. High ESV areas shifted from southwest to central then northern regions, driven by mining subsidence, land restoration, urbanization, and policies. This research is essential for comprehending the implications of coal mining subsidence, offering insights into land resource conservation, as well as rational and sustainable development of regional ecological services.

**Keywords:** *land use and land cover changes (LUCC), landscape pattern index, driving factor, land restoration, policy drivers*

## Introduction

Coal remains the predominant energy source in China, constituting over 50% of the nation's total energy consumption and playing a critical role in both economic and social development (The National Bureau of Statistics of the People's Republic of China, 2022; Zhao et al., 2014; Xiao et al., 2018). In 2021, China's coal production reached 41.26 billion tons, accounting for 50.48% of global coal output (The National Bureau of Statistics of the People's Republic of China, 2022). The significance of coal resources has led to the emergence of numerous coal-dependent cities in the eastern plains of China (Xiao et al., 2018; Han et al., 2022; Song et al., 2022; Zhou et al., 2022; Yan et al., 2023; Li et al., 2023; Zhou, 2022). Notably, over 92% of coal in China is extracted through underground mining, a practice that inevitably results in extensive land subsidence. Research indicates that approximately 20 to 33 ha of land subsides for every million tons of coal mined underground, with subsidence areas expanding by 20,000 ha annually across the country (Hu et al., 2013). Additionally, coal resource-based cities in China typically feature multiple and thick coal seams, elevated


http://www.aloki.hu ● ISSN 1589 1623 (Print) ● ISSN 1785 0037 (Online)
DOI: http://dx.doi.org/10.15666/aeer/2305_91019120

groundwater tables, and flat topography, which exacerbate the consequences of subsidence, leading to significant farmland destruction and extensive waterlogging, with depths exceeding 20 m in certain regions (Liu et al., 2021). The ongoing subsidence associated with coal mining alters land use patterns, disrupts ecosystem functions, and poses threats to ecosystem services. Furthermore, the rapid urbanization in China since the early 21st century has resulted in the continuous expansion of urban areas, bringing coal mining regions increasingly closer to urban centers. This phenomenon has led to the problematic situation of "cities surrounded by subsidence land." A notable case is Jining City, which, as of 2021, has experienced 450.94 $km^2$ of subsidence land, with over ten coal mines situated in proximity to the urban core, thereby severely limiting available space for urban development. Consequently, there is an urgent need for the reclamation and restoration of subsided land.

Ecosystem services encompass both the evident and potential advantages that individuals derive from ecosystems, which are crucial for human well-being and the sustainable advancement of economic and societal development. These services can be categorized into four primary types: provisioning services (PS), regulating services (RS), supporting services (SS), and cultural services (CS) (Daily, 1997). In 1997, Costanza (Constanza et al., 1997) introduced a foundational methodology for assessing ecosystem service value (ESV) grounded in equilibrium value theory. This framework has since been extensively utilized to evaluate the interactions between human societies and natural ecosystems (Adhikari and Hartemink, 2016). The United Nations Millennium Assessment (MEA, 2005) highlighted that land use and land cover changes (LUCC) have resulted in the degradation of nearly 60% of ecosystems, primarily due to anthropogenic activities (United Nations, 2001). In China, Xie developed the "Chinese terrestrial ecosystem service value equivalent factor table" (Xie et al., 2003, 2005, 2008), which is based on Costanza's methodology and has garnered significant attention from both academic and policy-making circles. Although the methodologies proposed by Costanza and Xie exhibit limitations in accurately estimating ecosystem services, they effectively reflect changes in ESV across extensive areas over time (Li et al., 2020). Given that our research focuses on the temporal changes in ecosystem services influenced by coal mining subsidence, the estimation of ESV that emphasizes trends was sufficient. The methods and parameters established by Xie et al. were selected for their greater applicability to ESV assessments in China. Recent advancements in ESV methodologies have predominantly concentrated on developed regions with comprehensive social statistics (Ma et al., 2023; Yang et al., 2023; Zhang et al., 2022) or natural ecosystems that are largely undisturbed by human activities (Zhang et al., 2023a, b). However, areas affected by coal mining subsidence, characterized by frequent land use changes and significant human activity, have received insufficient attention, indicating a need for further research.

This study specifically examines the coal mining subsidence regions in the Taibai Lake District of Jining City (MSTL), which is designated as the planned core urban area of the city. The objectives of this research are threefold: (1) to analyze land use changes in MSTL from 2000 to 2021; (2) to estimate the ESV, considering the specific conditions and land use changes in MSTL; and (3) to identify the primary driving factors behind changes in ESV and to propose recommendations for land use management, urban development, and ecological protection of coal mining subsidence areas in China.


http://www.aloki.hu ● ISSN 1589 1623 (Print) ● ISSN 1785 0037 (Online)
DOI: http://dx.doi.org/10.15666/aeer/2305_91019120

## Overview of the study area

The Taibai Lake District (TLD) is situated in the southern part of the central urban area of Jining City, Shandong Province, with geographical coordinates ranging from 35°15′ to 35°20′ N and 116°36′ to 116°42′ E (*Fig. 1*). This region is characterized by a dense network of rivers, efficient transportation systems, an aesthetically pleasing natural environment, and distinctive ecological attributes. Additionally, TLD is adjacent to Nansi Lake, which is recognized as the largest freshwater lake in northern China. The district encompasses a sub-district, Xuzhuang Street, and a town, Siqiao Town, covering a total land area of 133 km$^2$ and supporting a population of approximately 120,000 residents.

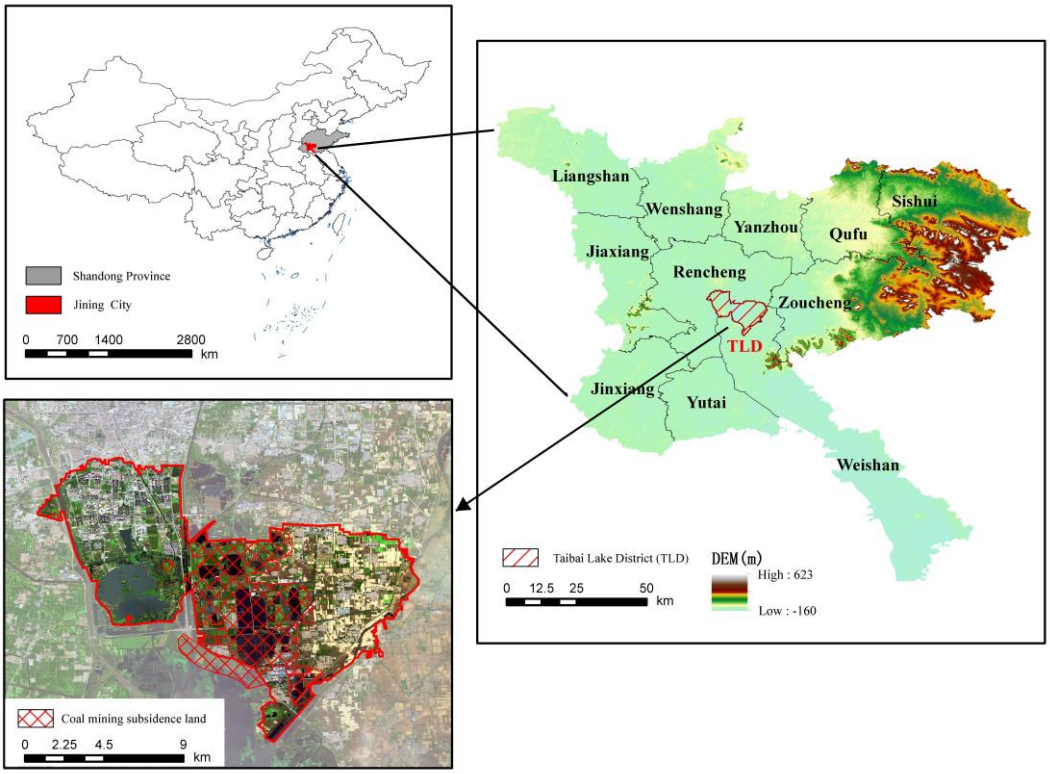


***Figure 1.*** *Location map of study area. Maps of Jining City in Shandong Province of China (A) and of parts of Taibai Lake District (TLD) in Jining City (B). C is a map of coal mining subsidence in Taibai Lake District (MSTL)*

The TLD region is characterized by substantial coal reserves, with an estimated 895 million tons identified and 758 million tons retained as of the year 2020. The area designated for coal distribution encompasses approximately 70% of the total region. Within this area, two coal mines are operated by Yankuang Energy Group Co., Ltd.: the Jining No.2 Coal Mine (No.2 CM) and the Jining No.3 Coal Mine (No.3 CM). The mining areas for No.2 CM and No.3 CM are 87.11 km² and 105.05 km², respectively, with the primary mineral seam being the 3# coal seam, which has an average thickness exceeding 6 m. The No.2 CM commenced official operations in November 1997, with an annual production capacity of 4.2 million tons, while the No.3 CM began operations in December 2000, with a capacity of 6 million tons per year.


http://www.aloki.hu ● ISSN 1589 1623 (Print) ● ISSN 1785 0037 (Online)
DOI: http://dx.doi.org/10.15666/aeer/2305_91019120

This study focuses on the MSTL area as of 2021, which is depicted in *Figure 1* and spans 3833.16 ha, representing 28.82% of the total district area. It is noteworthy that the southwestern portion of the MSTL is located in Weishan County, which has been allocated to TLD to support the reclamation and restoration efforts for subsided land.

## Data sources and research methods

### *Data sources and process*

To examine the alterations in Ecosystem Service Value (ESV) resulting from mining activities in the MSTL region, remote sensing imagery from Landsat-5 TM for the years 2000, 2004, 2009, and 2013, as well as Landsat-8 OLI for the years 2016, 2018, and 2021, was utilized. The imagery for each time period consisted of mosaics created from two specific images (P112R35 and P112R36), which were sourced from the Geospatial Data Cloud (https://www.gscloud.cn) and selected based on a cloud cover percentage of less than 10%.

In alignment with the land use characteristics observed in TLD, land use maps spanning from 2000 to 2021 were categorized into five distinct types: farmland, forest land, grassland, water bodies, and constructed land (which encompasses industrial, mining, transportation, and settlement areas) (Xiao et al., 2018). The data underwent preprocessing using ENVI software, which included radiometric calibration, atmospheric correction, image enhancement, and cropping. Initial results were derived through supervised classification interpretation employing support vector machine methodologies. Subsequently, these results were refined using land use change survey data, leading to the compilation of the final land use maps. Validation tests indicated that the Kappa coefficients exceeded 80%.

Additionally, economic and social data were gathered from the Jining City statistical yearbook, the National Bureau of Statistics' national data website, and various local government departments.

### *Land use dynamic degree*

Land use dynamic degree is an important parameter, which widely used to quantitatively describe the rate and intensity of land use change, including single land use dynamic degree ($K$) and comprehensive land use dynamic degree ($LC$) (Redo et al., 2012).

$$K = \frac{U_b - U_a}{U_a} \times \frac{1}{T} \times 100\% \quad \text{(Eq.1)}$$

$$LC = \frac{\sum_{i=1}^{n} \Delta LU_{i-j}}{2LU} \times \frac{1}{T} \times 100\% \quad \text{(Eq.2)}$$

where $K$ is the dynamic degree of a certain land use type, and $LC$ is the comprehensive land use dynamic degree. $U_a$ and $U_b$ represent the area of the land use type at the beginning and end of a certain study period, respectively. $LU$ is the total area of the study area. $\Delta LU_{i-j}$ is the absolute value of the area of land use type $i$ transfer to land use type $j$ ($i \neq j$) during a certain study period. T is the study period.


http://www.aloki.hu ● ISSN 1589 1623 (Print) ● ISSN 1785 0037 (Online)
DOI: http://dx.doi.org/10.15666/aeer/2305_91019120

### *Land use transfer matrix*

The land use transfer matrix can be used to calculate the area of interconversion between different land use types, which describe the changes in quantity and structure of land use types to reflect the process of land use change during the study time (Berihun et al., 2019). It can be expressed as:

$$S_{ij} = \begin{bmatrix} S_{11} & \cdots & S_{1n} \\ \vdots & \vdots & \vdots \\ S_{n1} & \cdots & S_{nn} \end{bmatrix} \quad \text{(Eq.3)}$$

where $S_{ij}$ represents the area; $n$ is the number of types of land use.

### *Landscape pattern index*

The landscape pattern index, a concentrated quantitative measure of landscape information, is extensively utilized to elucidate the dynamic processes associated with changes in landscape patterns (Liu and Zhou, 2021; Liu et al., 2015; Qian et al., 2023). This study employs various class metrics, including the largest patch index (LPI), edge density (ED), landscape shape index (LSI), and patch cohesion index (COHESION), alongside landscape metrics such as Shannon's Diversity Index (SHDI), Shannon's Evenness Index (SHEI), aggregation index (AI), and contagion index (CONTAG). These metrics have been selected to effectively represent the characteristics of the landscape patterns within the study area. The calculation method for the landscape pattern index mentioned above is as follows.

$$LPI = \frac{a_{\max}}{A} \times 100 \quad \text{(Eq.4)}$$

$$ED = \frac{E}{A} \times 10^6 \quad \text{(Eq.5)}$$

$$LSI = \frac{0.25E}{\sqrt{A}} \quad \text{(Eq.6)}$$

where $a_{max}$ represents the area of the largest patch; $E$ is the product of the number of grid boundaries of patches and the side length of grid units; $A$ is the total landscape area.

$$COHESION = \left(1 - \sum_{j=1}^{n} \frac{p_{ij}}{\sum_{j=1}^{n} \sqrt{a_{ij}}}\right)\left(1 - \frac{1}{\sqrt{A}}\right)^{-1} \times 100 \quad \text{(Eq.7)}$$

where $n$ is the total number of patch types; $p_{ij}$ is the perimeter of the $j$ patch in the $i$ landscape; $a_{ij}$ is the area of the $j$ patch in the $i$ landscape; $A$ is the total landscape area

$$AI = \frac{g_{ij}}{\max \rightarrow g_{ij}} \times 100 \quad \text{(Eq.8)}$$

where $g_{ij}$ is the number of similar adjacent patches of corresponding landscape types.


http://www.aloki.hu ● ISSN 1589 1623 (Print) ● ISSN 1785 0037 (Online)
DOI: http://dx.doi.org/10.15666/aeer/2305_91019120

$$CONTAG = \left(1 + \sum_{i=1}^{n}\sum_{j=1}^{n}\frac{P_{ij}\ln(P_{ij})}{2\ln(n)}\right)\times 100 \quad \text{(Eq.9)}$$

$$SHDI = -\sum_{i=1}^{n}\left[P_i \ln(P_i)\right] \quad \text{(Eq.10)}$$

$$SHEI = \frac{-\sum_{i=1}^{n}(P_i \ln P_i)}{\ln n} \quad \text{(Eq.11)}$$

where $n$ is the total number of patch types; $P_{ij}$ is the probability of randomly two adjacent grid cells belonging to type $i$ and $j$.

### *Approaches to ESV*

To represent the spatial distribution and variations of Ecosystem Service Value (ESV) more accurately, we utilized the equivalent factor model for ESV as proposed by Xie et al. (2008). It is noteworthy that the water body was adjusted to reflect the average value of its respective water bodies and rivers/lakes. Additionally, since the equivalent factor for construction land is designated as zero (Yu et al., 2021), the ESV associated with construction land was excluded from this analysis. The regional adjustment coefficient for Shandong Province is established at 1.38 (Xie et al., 2005), and the average grain output for Jining City is 1.18 times that of Shandong Province. Consequently, the service value coefficient for the farmland ecosystem in the TLD region is 1.63 times the national average for China. Furthermore, based on the net profit from grain production per hectare of farmland ecosystem, which serves as the standard equivalent (Sutton and Constanza, 2002), the economic value of the equivalent factor in MSTL was calculated to be 2236.07 CNY/hm², utilizing local data from 2021. Thus, a base equivalent factor table relevant to the study area was developed (see *Table 1*).

***Table 1.*** *ESV equivalent factors table for different land use types in MSTL (units: CNY/hm$^2$)*

| Ecosystem services types | | Farmland | Forested land | Grassland | Water body | Construction land |
|---|---|---|---|---|---|---|
| Provision services (PS) | Food production | 4295.85 | 1417.63 | 1847.21 | 1911.65 | 0 |
| | Raw material production | 1675.38 | 12801.63 | 1546.51 | 1267.28 | 0 |
| Regulation services (RS) | Gas regulation | 3093.01 | 18558.07 | 6443.77 | 6271.94 | 0 |
| | Climate regulation | 4166.97 | 17484.10 | 6701.52 | 33529.10 | 0 |
| | Hydrological regulation | 3307.80 | 17570.02 | 6529.69 | 69184.64 | 0 |
| | Waste treatment | 5971.23 | 7388.86 | 5670.52 | 62826.79 | 0 |
| Support services (SS) | Soil conservation | 6314.90 | 17269.31 | 9622.70 | 5155.02 | 0 |
| | Biodiversity | 4381.77 | 19374.28 | 8033.24 | 15293.22 | 0 |
| Cultural services (CS) | Aesthetic landscape | 730.29 | 8935.37 | 3737.39 | 19610.55 | 0 |
| Total | | 33937.20 | 120799.27 | 50132.55 | 215050.19 | 0 |

The ESV can be calculated as following:

$$ESV = \sum_{i=1}^{n}(Ak \times VCk) \quad \text{(Eq.12)}$$


http://www.aloki.hu ● ISSN 1589 1623 (Print) ● ISSN 1785 0037 (Online)
DOI: http://dx.doi.org/10.15666/aeer/2305_91019120

$$ESV_f = \sum_{i=1}^{n} (A_k \times VC_{fk}) \quad \text{(Eq.13)}$$

where $ESV$ and $ESV_f$ are the total value of ecosystem services and the value of the $f$ service function type, respectively. $A_k$ represents the area of land use type $k$. $VC_k$ and $VC_{fk}$ are the ecosystem service value coefficient of land use type $k$ and the value coefficient of service function type $f$, respectively.

### *Grey relational degree model*

The grey relational degree model illustrates the geometric relationships among various discrete sequences, including reference sequences and at least one comparative sequence within the system. This model is employed to identify the primary driving factors influencing the evolution of Ecosystem Service Value (ESV) in Mountainous and hilly areas. The grey comprehensive correlation degree is defined as follows:

$$\rho_{0i} = \theta\varepsilon_{0i} + (1-\theta)\gamma_{0i} \quad \text{(Eq.14)}$$

where $\rho_{0i}$ is the grey comprehensive correlation degree; $\theta$ is the reference value, $\theta \in [0, 1]$, set at 0.5 in this study. $\varepsilon_{0i}$ and $\gamma_{0i}$ are the grey absolute correlation degree and the grey relative correlation degree, respectively.

The relevant indicators were performed in Grey System Theory Modeling Software (GSTA V7.0).

## Results

### *Land use change*

Through a comparative and overlay analysis of land use maps, the spatiotemporal distribution and changes in land use within the MSTL region from 2000 to 2021 were assessed (see *Tables 2* and *3; Fig. 2*). Overall, the land use structure during the study period was predominantly characterized by farmland and water bodies, which collectively accounted for between 77% and 96% of the total land use. This was followed by construction land, while the combined percentages of forest and grassland were consistently below 5%. Regarding land use change, the comprehensive land use dynamic degree (LC) from 2000 to 2021 was recorded at 1.01%. Notably, the LC value exhibited a decline from 1.94% at T1 to 0.93% at T3, subsequently peaking at 2.86% at T4 before dropping to a minimum of 0.29%, and finally stabilizing at 1.54% at T6. These findings indicate a period of frequent and significant land use changes in MSTL, accompanied by a gradual reduction in the intensity of such changes over the study duration.

The area of farmland experienced a decline of 2042.59 ha from 2000 to 2018, exhibiting a single land use dynamic degree (K) of -3.44%. This decline resulted in farmland transitioning from the predominant land use type to the second position between 2016 and 2018 within the MSTL framework. However, in 2021, there was a significant increase of 458.89 ha, with a K value of 12.17%, allowing farmland to regain its status as the primary land use type. Conversely, the area designated for water bodies increased by 1381.73 ha from 2000 to 2018, with a K value of 22.42%,


http://www.aloki.hu ● ISSN 1589 1623 (Print) ● ISSN 1785 0037 (Online)
DOI: http://dx.doi.org/10.15666/aeer/2305_91019120

surpassing farmland to become the largest land use type from 2016 to 2018. In 2021, growth in water body area was curtailed, resulting in a decrease of 121.58 ha and a K value of -2.35%, thus reverting to the second position. The area allocated for construction land expanded significantly from 67.08 ha in 2000 to 280.61 ha in 2016, with a K value of 19.90%, and subsequently stabilized above 280 ha. The areas of forest land and grassland exhibited considerable fluctuations; the total area of forest land increased from 31.13 ha in 2000 to 156.80 ha in 2021, with a K value of 19.22%, while grassland decreased from 93.24 ha in 2000 to 76.22 ha in 2021, reflecting a K value of -0.87%. Furthermore, an analysis of the land use transfer matrix (*Table 4; Fig. 3*) reveals that the most significant trends in land use change include the continued decrease and subsequent increase of farmland, the initial increase followed by a decrease in water bodies, and the substantial reduction in farmland area primarily attributed to the expansion of water bodies and the encroachment of construction land, resulting in losses of 1402.99 $hm^2$ and 382.96 $hm^2$, respectively.

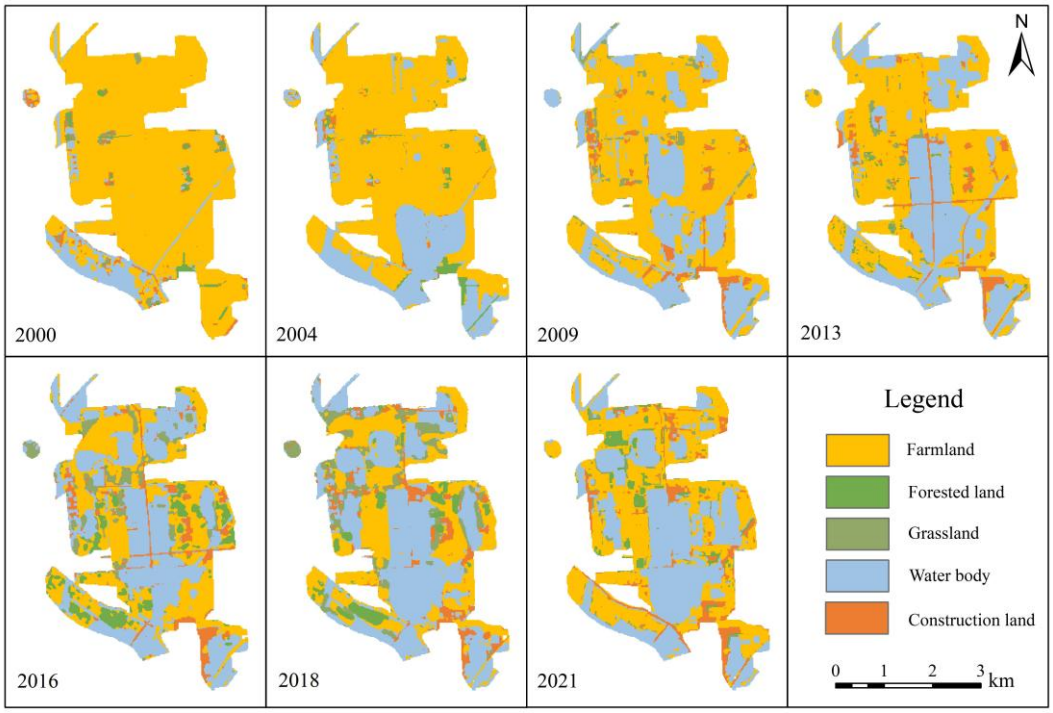


***Figure 2.*** *Spatial distribution of land use in the study area from 2000 to 2021*

***Table 2.*** *Land use area and percentages of MSTL from 2000 to 2021 (units: $hm^2$, %)*

| Year | Area and percentages | | | | | | | | | |
|---|---|---|---|---|---|---|---|---|---|---|
| | Farmland | | Forested land | | Grassland | | Water body | | Construction land | |
| 2000 | 3299.31 | 86.07 | 31.13 | 0.81 | 93.24 | 2.43 | 342.40 | 8.93 | 67.08 | 1.75 |
| 2004 | 2735.10 | 71.35 | 16.32 | 0.43 | 45.29 | 1.18 | 942.76 | 24.59 | 93.69 | 2.44 |
| 2009 | 2349.25 | 61.29 | 33.43 | 0.87 | 102.54 | 2.68 | 1148.22 | 29.95 | 199.72 | 5.21 |
| 2013 | 2080.13 | 54.27 | 47.71 | 1.24 | 64.51 | 1.68 | 1407.17 | 36.71 | 233.65 | 6.10 |
| 2016 | 1403.74 | 36.62 | 266.86 | 6.96 | 258.00 | 6.73 | 1623.97 | 42.37 | 280.61 | 7.32 |
| 2018 | 1256.72 | 32.79 | 180.19 | 4.70 | 387.50 | 10.11 | 1724.13 | 44.98 | 284.62 | 7.43 |
| 2021 | 1715.61 | 44.76 | 156.80 | 4.09 | 76.22 | 1.99 | 1602.55 | 41.81 | 281.98 | 7.36 |


http://www.aloki.hu ● ISSN 1589 1623 (Print) ● ISSN 1785 0037 (Online)
DOI: http://dx.doi.org/10.15666/aeer/2305_91019120

***Table 3.*** *Land use dynamic degree (LC and K) of MSTL*

| Land use types | K | | | | | LC |
|---|---|---|---|---|---|---|
| | Farmland | Forested land | Grassland | Water body | Construction land | |
| 2000–2004 (T1) | -4.28% | -11.89% | -12.86% | 43.83% | 9.92% | 1.94% |
| 2004–2009 (T2) | -2.82% | 20.97% | 25.28% | 4.36% | 22.63% | 1.12% |
| 2009–2013 (T3) | -2.86% | 10.68% | -9.27% | 5.64% | 4.25% | 0.93% |
| 2013–2016 (T4) | -10.84% | 153.10% | 99.98% | 5.14% | 6.70% | 2.86% |
| 2016–2018 (T5) | -5.24% | -16.24% | 25.10% | 3.08% | 0.71% | 0.29% |
| 2018–2021 (T6) | 12.17% | -4.33% | -26.78% | -2.35% | -0.31% | 1.54% |
| 2000–2021 | -2.29% | 19.22% | -0.87% | 17.53% | 15.26% | 1.01% |

***Table 4.*** *Land use transfer matrix of MSTL*

| Period | Land use types | Farmland | Forested land | Grassland | Water body | Construction land |
|---|---|---|---|---|---|---|
| 2000–2004 | Farmland | 2539.73 | 17.94 | 49.66 | 109.33 | 18.45 |
| | Forested land | 7.82 | 4.55 | 0.36 | 1.46 | 2.13 |
| | Grassland | 27.68 | 1.18 | 6.12 | 5.83 | 4.48 |
| | Water body | 684.28 | 4.74 | 28.17 | 219.06 | 6.51 |
| | Construction land | 39.81 | 2.72 | 8.94 | 6.72 | 35.51 |
| 2004–2009 | Farmland | 2086.29 | 8.63 | 17 | 211.32 | 26.01 |
| | Forested land | 23.11 | 2.21 | 0.72 | 7 | 0.39 |
| | Grassland | 71.94 | 1.5 | 6.53 | 22.18 | 0.4 |
| | Water body | 476.75 | 2.66 | 12.56 | 641.34 | 14.9 |
| | Construction land | 77 | 1.32 | 8.49 | 60.92 | 51.99 |
| 2009–2013 | Farmland | 1764.4 | 20.61 | 63.81 | 173.57 | 57.73 |
| | Forested land | 39.17 | 0.25 | 1.67 | 5.15 | 1.47 |
| | Grassland | 47.47 | 0.98 | 2.33 | 11.44 | 2.29 |
| | Water body | 403.7 | 9.52 | 27 | 909.73 | 57.21 |
| | Construction land | 94.52 | 2.06 | 7.72 | 48.32 | 81.02 |
| 2013–2016 | Farmland | 1154.99 | 22 | 28.74 | 151.99 | 46.02 |
| | Forested land | 231.8 | 9.47 | 3.64 | 20.27 | 1.68 |
| | Grassland | 211.26 | 5.3 | 10.24 | 25.8 | 5.4 |
| | Water body | 388.06 | 8.97 | 17.24 | 1158.16 | 51.53 |
| | Construction land | 94.02 | 1.97 | 4.65 | 50.95 | 129.02 |
| 2016–2018 | Farmland | 872.98 | 127.68 | 105 | 100.97 | 50.1 |
| | Forested land | 64.7 | 79.42 | 17.73 | 13.34 | 5 |
| | Grassland | 150.68 | 11.49 | 82.16 | 120.03 | 23.13 |
| | Water body | 216.9 | 44.54 | 36.83 | 1354.21 | 71.64 |
| | Construction land | 98.48 | 3.72 | 16.27 | 35.41 | 130.73 |
| 2018–2021 | Farmland | 967.69 | 125.36 | 257.18 | 235.53 | 129.85 |
| | Forested land | 93.73 | 22.69 | 17.2 | 8.71 | 14.46 |
| | Grassland | 25.57 | 3.29 | 20.46 | 16.78 | 10.12 |
| | Water body | 86.37 | 25.25 | 75.79 | 1392.55 | 22.59 |
| | Construction land | 83.36 | 3.6 | 16.87 | 70.56 | 107.59 |
| 2000–2021 | Farmland | 1461.42 | 21.05 | 59.35 | 138.33 | 35.46 |
| | Forested land | 142.85 | 2.92 | 3.25 | 1.33 | 6.45 |
| | Grassland | 63.92 | 0.72 | 2.02 | 7.65 | 1.92 |
| | Water body | 1414.75 | 4 | 15.86 | 164.46 | 3.49 |
| | Construction land | 216.37 | 2.45 | 12.77 | 30.63 | 19.76 |


http://www.aloki.hu ● ISSN 1589 1623 (Print) ● ISSN 1785 0037 (Online)
DOI: http://dx.doi.org/10.15666/aeer/2305_91019120

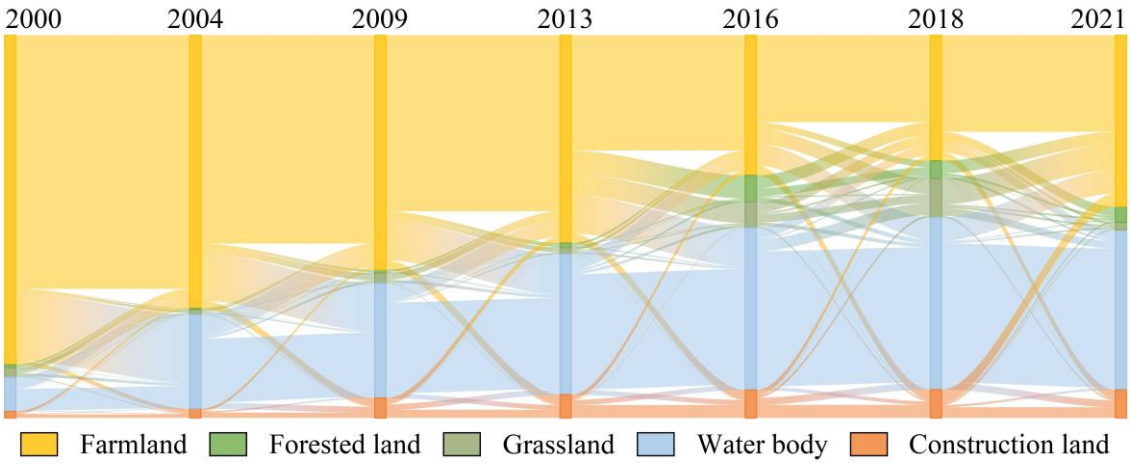


***Figure 3.*** *Land use change of MSTL from 2000 to 2021*

## *Characteristics of landscape pattern*

There are multiple landscape pattern indexes in one aspect of landscape pattern characteristics. In order to reflect the characteristics of landscape pattern as much as possible and avoid data redundancy, the selection and analysis results of landscape pattern indexes were presented in *Figure 4* and *Table 5*.

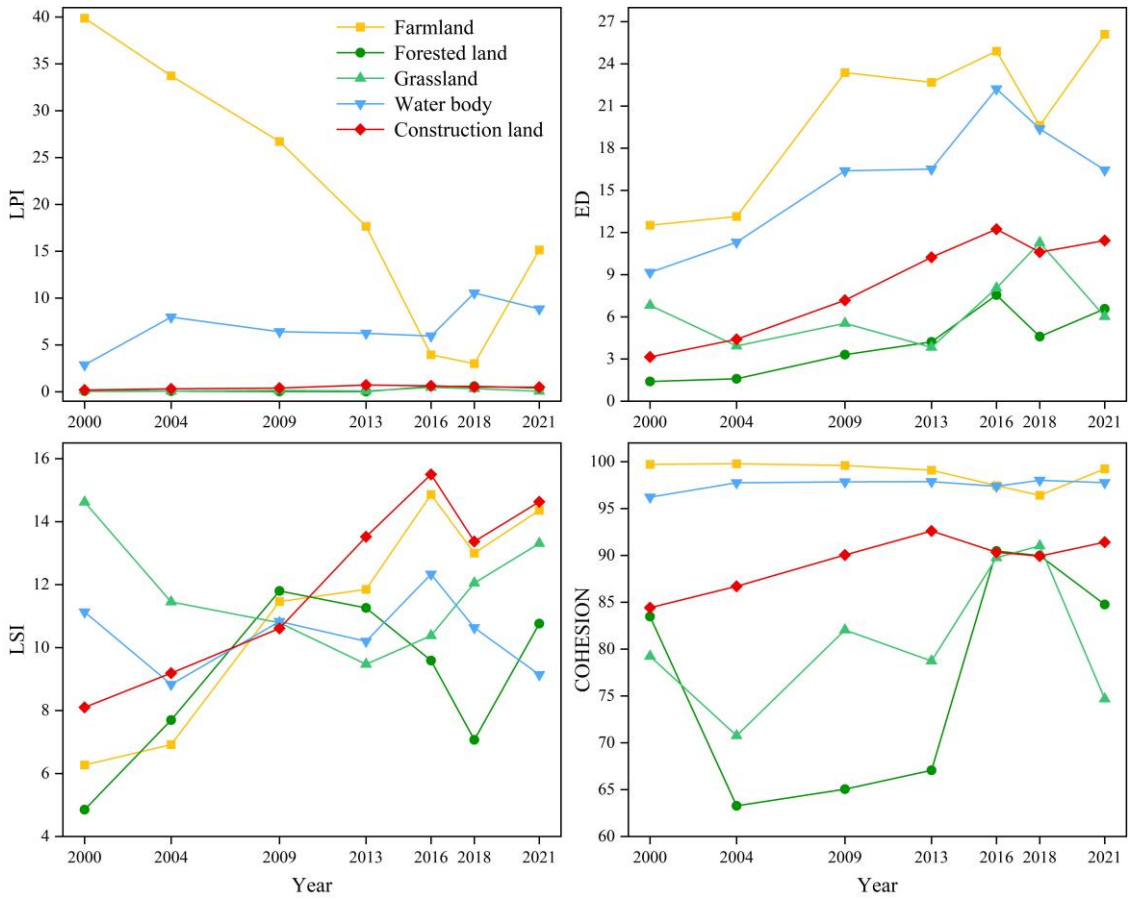


***Figure 4.*** *Landscape pattern index at class metrics level of MSTL from 2000 to 2021*

APPLIED ECOLOGY AND ENVIRONMENTAL RESEARCH 23(5):9101-9120.
http://www.aloki.hu ● ISSN 1589 1623 (Print) ● ISSN 1785 0037 (Online)
DOI: http://dx.doi.org/10.15666/aeer/2305_91019120

***Table 5.*** *Landscape pattern index at landscape metrics level of MSTL from 2000 to 2021*

| Year | AI | CONTAG | SHDI | SHEI |
|---|---|---|---|---|
| 2000 | 94.38 | 75.88 | 0.56 | 0.35 |
| 2004 | 94.44 | 70.54 | 0.73 | 0.45 |
| 2009 | 91.00 | 59.20 | 0.96 | 0.59 |
| 2013 | 95.58 | 61.79 | 1.15 | 0.64 |
| 2016 | 93.42 | 54.13 | 1.34 | 0.75 |
| 2018 | 93.92 | 54.45 | 1.34 | 0.75 |
| 2021 | 94.41 | 58.02 | 1.24 | 0.69 |

### *Characteristics of landscape pattern index at class metrics level*

The Largest Patch Index (LPI) quantifies the proportion of the largest patch area within a given landscape, serving as an indicator of landscape dominance and the influence of anthropogenic activities (Deng et al., 2015). Throughout the study period, the LPI for agricultural land consistently exhibited a notable advantage over other land use categories, except for the years 2016 and 2018. However, this advantage demonstrated a pattern of rapid decline followed by a subsequent increase, with the overall extent of the decrease being substantial. The LPI for aquatic environments displayed a fluctuating upward trend, ranking second to agricultural land, and surpassing it in the years 2016 and 2018. In contrast, the LPI values for constructed areas, forested land, and grasslands were comparatively lower.

Edge Density (ED) measures the extent of landscape fragmentation caused by boundaries (Sutton and Constanza, 2002). A higher ED value indicates more complex patch shapes and a greater degree of segmentation. During the study period, the ED values for agricultural land, aquatic environments, and constructed areas exhibited a tiered increase, with agricultural land having the highest ED, reflecting a significant level of landscape fragmentation and spatial heterogeneity. This was followed by aquatic environments and constructed areas. Conversely, the ED for forested land remained relatively stable at a lower level, while grassland ED showed a declining trend, indicating a reduced degree of landscape fragmentation and spatial heterogeneity, as well as a greater susceptibility to human disturbances.

The Landscape Shape Index (LSI) serves as a metric for assessing the complexity of patch shapes within a landscape; a higher LSI value signifies greater intricacy, whereas a lower value indicates a more simplistic landscape configuration (Sun et al., 2022). Observations reveal an upward trend in the LSI values for both construction land and farmland, with construction land surpassing farmland in complexity from 2013 onwards, suggesting an overall increase in landscape complexity. Conversely, the LSI for water bodies has exhibited fluctuations around a value of 10, demonstrating a recent decline in complexity, which suggests a movement towards a more holistic and expansive landscape. The LSI for forest land has experienced two fluctuations, ultimately decreasing to its lowest level recorded in 2000 by 2021, while the LSI for grassland has also shown a downward trend, indicating a simplification in the complexity of their respective patch shapes.

The Patch Cohesion Index (COHESION) quantifies the connectivity among various landscape types and the physical connectivity of patches. A higher


http://www.aloki.hu ● ISSN 1589 1623 (Print) ● ISSN 1785 0037 (Online)
DOI: http://dx.doi.org/10.15666/aeer/2305_91019120

COHESION value reflects stronger landscape connectivity (Hu et al., 2022). Both farmland and water bodies have maintained high COHESION values, exceeding 96, which indicates optimal natural connectivity. The COHESION value for construction land has demonstrated a significant upward trajectory, increasing from 79.11 in 2000 to 94.63 in 2021, thereby aligning with the values of farmland and water bodies and indicating a marked improvement in connectivity for construction land. The trends observed in forest land and grassland are more complex, characterized by a pattern of decrease-increase-decrease, with the 2021 values approximating those of 2000. Notably, the COHESION value for forest land (88.23) surpasses that of grassland (65.74), suggesting superior connectivity for forest land compared to grassland.

### *Characteristics of landscape pattern index at landscape metrics level*

The Aggregation Index (AI), Contagion Index (CONTAG), Shannon's Diversity Index (SHDI), and Shannon's Evenness Index (SHEI) serve as metrics for assessing the connectivity, fragmentation, heterogeneity, and evenness of landscapes, respectively (Hu et al., 2022). Between the years 2000 and 2016, the AI remained consistently above 90, while the CONTAG experienced a decline of 28.66%. In contrast, both the SHDI and SHEI exhibited increases of 1.38 times and 1.14 times, respectively, signifying a notable enhancement in landscape heterogeneity. This period was characterized by a reduction in spatial aggregation and connectivity, alongside a trend towards greater diversification and uniformity in landscape distribution. However, from 2016 to 2021, the AI continued to stabilize above 90, and the CONTAG showed a slight upward trend. Conversely, both the SHDI and SHEI experienced minor declines, indicating a slight reduction in the fragmentation, uniformity, and diversity of the landscape. This shift suggests a gradual improvement in the spatial aggregation and connectivity of the landscape pattern in recent years.

In conclusion, the land use patterns within MSTL underwent significant transformations throughout the study period. The predominant land use categories included farmland and water bodies, followed by construction land, forest land, and grassland. Initially, farmland experienced a continuous increase, which was subsequently followed by a decline; a similar trend was observed for water bodies. The primary land use transitions involved the conversion of farmland to water bodies, with a secondary transition from farmland to construction land. Between 2000 and 2016, the landscape exhibited characteristics of fragmentation, uniformity, and diversification. However, from 2016 to 2021, there was a noticeable reduction in the levels of fragmentation, uniformity, and diversity, indicating a gradual optimization of the landscape pattern.

### *Spatiotemporal variation of ESV*

#### *Temporal evolution of ESV*

As illustrated in *Table 6,* the total Ecosystem Service Value (ESV) in MSTL exhibited a continuous increase from 194.04 million CNY in 2000 to 454.62 million CNY in 2018, representing more than a twofold increase. However, this value experienced a slight decline to 425.62 million CNY in 2021, accompanied by a generally decreasing average annual growth rate (r) throughout the study period. Analyzing various ecosystem types reveals that water bodies were the predominant


http://www.aloki.hu ● ISSN 1589 1623 (Print) ● ISSN 1785 0037 (Online)
DOI: http://dx.doi.org/10.15666/aeer/2305_91019120

contributors to ESV. The methodologies employed in this study, which included an examination of land use and ESV equivalent factors, indicate that the ESV associated with different land use types in MSTL displayed consistent patterns in relation to land use area. Notably, water bodies emerged as the largest contributor to the total ESV during the study period, except for the year 2000, attributable to their extensive area and elevated ESV equivalent factors. This was followed by farmland, while the contributions from forest land and grassland were comparatively lower.

***Table 6.*** *ESV of MSTL from 2000 to 2021 (units: 104 CNY, %)*

| Year | ESV and percentages | | | | | | | | Total ESV | r |
|---|---|---|---|---|---|---|---|---|---|---|
| | Farmland | | Forested land | | Grassland | | Water body | | | |
| 2000 | 11196.95 | 57.71 | 376.04 | 1.94 | 467.45 | 2.41 | 7363.31 | 37.95 | 19403.75 | / |
| 2004 | 9282.17 | 30.96 | 197.16 | 0.66 | 227.06 | 0.76 | 20274.07 | 67.62 | 29980.46 | 13.63 |
| 2009 | 7972.71 | 23.74 | 403.87 | 1.20 | 514.05 | 1.53 | 24692.40 | 73.53 | 33583.03 | 2.40 |
| 2013 | 7059.37 | 18.47 | 576.37 | 1.51 | 323.39 | 0.85 | 30261.15 | 79.18 | 38220.28 | 3.45 |
| 2016 | 4763.90 | 10.78 | 3223.63 | 7.29 | 1293.40 | 2.93 | 34923.43 | 79.00 | 44204.36 | 5.22 |
| 2018 | 4264.96 | 9.38 | 2176.74 | 4.79 | 1942.63 | 4.27 | 37077.52 | 81.56 | 45461.85 | 1.42 |
| 2021 | 5822.29 | 13.68 | 1894.18 | 4.45 | 382.14 | 0.90 | 34462.90 | 80.97 | 42561.50 | -2.13 |

*Spatial evolution of ESV*

The choice of evaluation scales significantly influences the spatial distribution of Ecosystem Service Value (ESV). Generally, a smaller evaluation unit yields a more accurate representation of ESV's spatial distribution. In alignment with the scale selection employed by other researchers and taking into account the dimensions of the study area, a grid scale of 250 m × 250 m was selected for the analysis of ESV's spatial evolution in MSTL. *Figure 5* illustrates the spatial distribution of ESV in MSTL from 2000 to 2021, categorized into five grades (I-V) using the natural breaks method in ArcGIS software, which reflects ESV levels ranging from low to high. The high ESV regions within the study area exhibited a progression from the southwest towards the center, subsequently extending northward between 2000 and 2021. In 2000, the ESV was predominantly low, with the peripheral areas exhibiting extremely low values, while the southwest region displayed high and extremely high ESV. By 2004, the area of high ESV began to expand southeastward, continuing its growth towards the center by 2009. In 2013, a connection was established between the central and southern regions characterized by high ESV. By 2016, high ESV was prevalent throughout the entire study area. The regions classified as high to extremely high ESV further expanded and converged towards the central area, whereas the medium ESV regions experienced a slight decline from 2018 to 2021.

*Grey correlation results between ESV and driving factors*

The grey correlation results between Ecosystem Service Value (ESV) and driving factors are shown in *Table 7*. The overall results are relatively high, all exceeding 0.5, and the highest can reach above 0.9. These specific correlation relationships will be analyzed and discussed in the following "Discussion" section.


http://www.aloki.hu ● ISSN 1589 1623 (Print) ● ISSN 1785 0037 (Online)
DOI: http://dx.doi.org/10.15666/aeer/2305_91019120

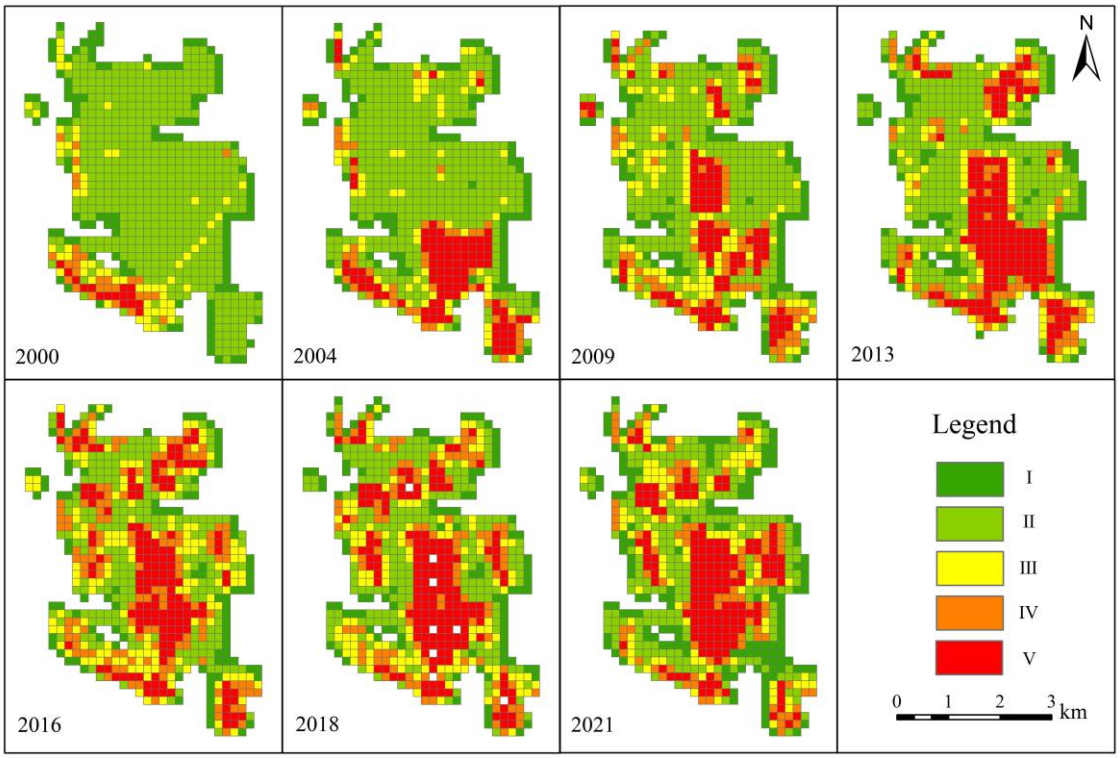


***Figure 5.*** *Spatial distribution of the total ESV in MSTL from 2000 to 2021*

***Table 7.*** *Grey relational degree between ESV and driving factors*

| Driving factors | PS | RS | SS | CS | ESV |
|---|---|---|---|---|---|
| UR | 0.5566 | 0.7003 | 0.5664 | 0.6379 | 0.7259 |
| SA | 0.5659 | 0.8696 | 0.5840 | 0.6492 | 0.9643 |
| RR | 0.5062 | 0.7080 | 0.5141 | 0.5377 | 0.7380 |
| AP | 0.7283 | 0.5327 | 0.6682 | 0.5316 | 0.5445 |
| AT | 0.6243 | 0.5224 | 0.6054 | 0.5155 | 0.5309 |

UR, urbanization rate; SA, subsidence area; RR, reclamation and restoration of mining subsidence; AP, annual precipitation; AT, annual temperature

## Discussion

### *Driving factor analysis*

#### *Urbanization development*

The findings regarding land use change indicate a significant increase in the area designated for construction within the MSTL, which may be attributed to the urbanization processes occurring within the city. Since the year 2000, coal resource-dependent cities in eastern China have undergone rapid urbanization, leading to a cessation in the expansion of construction land while a substantial amount of surrounding land has been appropriated. Specifically, the urbanization rate of Jining City rose from 23.79% in 2000 to 61.19% in 2021, with the urban area expanding from 30 km² to 248.94 km². Similarly, the construction land area in SATL experienced a notable increase from 67.08 hm² in 2000 to 280.61 hm² in 2016, subsequently


http://www.aloki.hu ● ISSN 1589 1623 (Print) ● ISSN 1785 0037 (Online)
DOI: http://dx.doi.org/10.15666/aeer/2305_91019120

stabilizing above 280 hm². Although the overall scale of construction land remains relatively small, it has nonetheless resulted in a degree of compression of space available for ecosystem services.

The results of the grey comprehensive correlation analysis (as presented in *Table 7*) reveal a moderate correlation between the urbanization rate (UR) and the total ecosystem service value (ESV), with a correlation coefficient exceeding 0.7. Additionally, a moderate correlation was observed between the urbanization rate and regulating services (RS), while the correlations with cultural services (CS), supporting services (SS), and provisioning services (PS) were found to be low, with values below 0.7. These findings suggest that urbanization is a significant driving factor influencing changes in ecosystem service values within the MSTL.

*Coal mining subsidence*

The analysis revealed that the area of water bodies resulting from coal mining subsidence in the MSTL exhibited a general upward trend, peaking in 2018. The coal production from No.2 CM and No.3 CM surpassed 10 million tons per year, leading to significant subsidence due to intensive mining operations. Furthermore, the presence of multiple and thick coal seams, a high groundwater table, and the overlap of agricultural land with coal resources contributed to the transformation of extensive farmland into water bodies, thereby inducing considerable changes in land use throughout the study period. Concurrently, the ongoing expansion of water bodies has encroached upon areas designated for urban development, particularly construction land, although this phenomenon has positively influenced the enhancement of ecosystem service value (ESV).

As illustrated in *Table 7,* a highly significant correlation was identified between the area of subsidence (SA) and the total ESV, with a correlation coefficient of 0.9643. This finding underscores the pivotal role of coal mining subsidence as a driving factor influencing changes in ESV within the MSTL. Additionally, the correlation between the area of subsidence and recreational services (RS) was found to be moderate, while the correlations with cultural services (CS), supporting services (SS), and provisioning services (PS) were relatively low, each exhibiting values below 0.7.

*Reclamation and restoration of subsidence land*

The conventional approach to the reclamation of subsidence land typically involves converting it back to agricultural use. However, the restoration of farmland on most subsidence land presents significant challenges due to factors such as high land utilization rates, a scarcity of suitable backfill materials for reclamation, and financial constraints. Prior to 2009, land reclamation efforts were largely characterized by spontaneous and small-scale initiatives. Between 2009 and 2018, local governments and coal mining companies undertook a series of land reclamation projects; although these efforts did not succeed in reversing the overall decline in farmland area, they did effectively mitigate the rate of decrease. In recent years, advancements in reclamation and restoration technologies have been actively pursued, leading to the implementation of dynamic reclamation projects that have sufficiently restored farmland. This has resulted in a notable "turnaround" in farmland area from 2018 to 2021. Concurrently, various ecological restoration projects have been initiated, which have contributed to the preservation of a secondary wetland ecosystem within the subsidence areas, characterized by a coordinated structure, optimal functionality, and robust self-maintenance of water bodies.


http://www.aloki.hu ● ISSN 1589 1623 (Print) ● ISSN 1785 0037 (Online)
DOI: http://dx.doi.org/10.15666/aeer/2305_91019120

The relationship between the area of reclaimed and restored subsidence land (RR) and the total ecosystem service value (ESV) was found to be moderately significant, with a correlation coefficient of 0.7380, surpassing the correlation between urban land (UR) and total ESV. This suggests that RR serves as a crucial driving factor influencing changes in ESV.

*Policy drivers*

Empirical research indicates that policy serves as a significant and often decisive factor influencing land use change, which subsequently impacts ecosystem service value (ESV) (Li et al., 2006). During the initial phase of this investigation, the regulatory influence of policies was relatively limited, resulting in minimal and ineffective land reclamation efforts in subsidence areas. The establishment of the Tianlong District (TLD) in 2008 marked a pivotal moment, as it was proposed to develop "the new ecological city." In 2009, TLD received approval to serve as the core urban area of Jining City, and by 2014, Shiqiao Town was incorporated into TLD. The issuance of the "Work Plan for Reclamation and Restoration of Coal Mining Subsidence in Shandong Province" in 2015 aimed to enhance reclamation and restoration efforts in subsidence regions. In recent years, there has been a concerted effort in China to strengthen farmland protection and ecological restoration, leading local governments to prioritize these initiatives in subsidence areas. Specifically, the implementation of policies such as "returning forest to farmland" and dynamic reclamation projects has aimed to optimize the protection and restoration of farmland. Concurrently, ecological restoration projects have transformed the previously homogeneous farmland ecosystem into a more integrated ecological framework characterized by diverse ecosystems, primarily dominated by agricultural land and aquatic environments. This transformation has positively contributed to ecological protection within TLD and the adjacent Nansi Lake Nature Reserve. Consequently, it can be concluded that policy drivers (PD) represent a significant factor influencing changes in ESV.

*Natural factors*

Temperature and precipitation, as primary natural factors, significantly influence the natural succession of ecosystems, exhibiting both cumulative and lag effects (He et al., 2010). Over the past two decades, the average annual precipitation in the study area has experienced considerable fluctuations; however, the multi-year average has remained stable, while the average annual temperature has demonstrated an upward trajectory. Consequently, the climate is characterized by a warming and drying trend. From a natural perspective, these alterations in temperature and precipitation are detrimental to the natural succession and development of vegetation. Nonetheless, the presence of a consistently high groundwater table and notable human intervention have resulted in a weak correlation between average precipitation (AP), average temperature (AT), and ecosystem service value (ESV), as indicated in *Table 7*. This suggests that the influence of natural factors on ESV changes is not substantial.

Based on the analysis of grey correlation degree, the five primary driving factors are ranked as follows: subsidence area (SA) > reclamation rate (RR) > urbanization rate (UR) > average precipitation (AP) > average temperature (AT). Among these factors, AP and AT are not regarded as significant drivers of ESV changes. Furthermore, while


http://www.aloki.hu ● ISSN 1589 1623 (Print) ● ISSN 1785 0037 (Online)
DOI: http://dx.doi.org/10.15666/aeer/2305_91019120

quantifying the impact of policy drivers is challenging, it is posited that their influence on ESV lies between UR and AP, as discussed previously. In summary, changes in ESV within the study area are predominantly driven by coal mining subsidence, the reclamation and restoration of subsided land, urbanization, and policy interventions. Specifically, from 2000 to 2018, urbanization resulted in a substantial increase in construction land, thereby constraining the availability of ecosystem services. Concurrently, ongoing coal mining subsidence led to a marked reduction in farmland area, while water bodies continued to expand. Given the extensive area of coal mining subsidence land, reclamation and restoration efforts have not reversed these trends, resulting in a continued increase in total ESV. From 2018 to 2021, however, the cumulative effects and ongoing optimization of reclamation and restoration efforts, coupled with effective policy guidance and constraints, facilitated an increase in farmland area and a decrease in water bodies, leading to a slight decline in total ESV.

### *Limitations and future work*

In this study, we did not consider the ecosystem service value (ESV) of construction land, assigning it a value of zero. However, the ESV associated with green belts within construction areas represents a significant component of the overall ESV and warrants further examination (Zhang et al., 2023c). Additionally, while necessary adjustments have been implemented, these modifications may only partially capture the complexities of the ecosystem's actual conditions. Furthermore, the ESV of land use types affected by subsidence differs from that of natural land use types; for instance, the ESV of subsidence-impacted farmland is lower than that of typical farmland. The underlying mechanisms contributing to this disparity have not been thoroughly elucidated and require further investigation.

### *Suggestions*

The findings of the research indicate that, despite a significant increase in total ecosystem service value (ESV), there has been a considerable reduction in farmland compared to 21 years ago, which poses a serious threat to food security. Concurrently, inadequate management of large-scale water bodies in subsiding areas may lead to the contamination of both surface and groundwater, the latter of which is particularly challenging to remediate. Furthermore, mining operations at sites No. 2 CM and No. 3 CM are projected to persist over the next decade, resulting in further subsidence. Consequently, to enhance the reclamation and restoration of subsided land and to foster high-quality spatial development in regions affected by coal mining subsidence, the following actions warrant increased attention: (1) The alignment of food security and ecosystem protection with regional urbanization efforts; (2) The innovation and implementation of reclamation and restoration technologies, such as concurrent mining and reclamation, to increase farmland area and stabilize grain production; and (3) The reinforcement of water body protection measures to minimize pollutant discharge and to prioritize biodiversity conservation.

## Conclusions

This study examines the phenomenon of coal mining subsidence in the eastern plain of China. Utilizing an analysis of land use changes alongside a grey relational degree


http://www.aloki.hu ● ISSN 1589 1623 (Print) ● ISSN 1785 0037 (Online)
DOI: http://dx.doi.org/10.15666/aeer/2305_91019120

model, the research investigates the evolution of land use and the driving factors influencing ecosystem service value (ESV) within the context of MSTL. The findings indicate that: (1) Farmland and water bodies represent the predominant land use types. The area designated for farmland initially experienced a decline, followed by a subsequent increase, while the area of water bodies exhibited an initial increase followed by a decrease. The primary land use transitions involved the conversion of farmland to water bodies, with a secondary transition from farmland to construction land. Between 2000 and 2016, the landscape exhibited an increase in fragmentation, uniformity, and diversity, which subsequently declined, indicating a gradual optimization of the landscape pattern from 2016 to 2021. (2) From 2000 to 2018, there was a significant increase in total ESV, which experienced a slight decrease in 2021. The distribution of high ESV shifted from the southwest to the central region, and then to the north of the study area, primarily influenced by factors such as coal mining subsidence, the restoration of subsided land, urban development, and policy interventions. This research is essential for comprehending the effects of coal mining subsidence and the associated reclamation and restoration efforts on subsided land, with important implications for land resource conservation, rational development, regional ecological protection, and sustainable development.

**Acknowledgments.** This study was supported by the Major Innovation Program of Jining City [grant number 2023HHCG003] and the Major Innovation Program of Shandong Province [grant number 2020CXC011403].

## REFERENCES

[1] Adhikari, K., Hartemink, A. E. (2016): Linking soils to ecosystem services—a global review. – Geoderma 262: 101-111. http://dx.doi.org/10.1016/j.geoderma.2015.08.009.

[2] Berihun, M. L., Tsunekawa, A., Haregeweyn, N., Meshesha, D. T., Adgo, E., Tsubo, M., Masunaga, T., Fenta, A. A., Sultan, D., Yibeltal, M. (2019): Exploring land use/land cover changes, drivers and their implications in contrasting agro-ecological environments of Ethiopia. – Land Use Policy 87: 104052. https://doi.org/10.1016/j.landusepol.2019.104052.

[3] Costanza, R., d'Arge, R., DeGroot, R., Farber, S., Grasso, M., Hannon, B., Llmburg, K., Naeem, S., V. O'Neill, R., Paruelo, J., G. Raskin, R., Sutton, P., Belt, M. (1997): The value of the world's ecosystem services and natural capital. – Nature 387(6630): 253-260.

[4] Daily, G. C. (1997): Nature's Service: Societal Dependence on Natural Ecosystems. 4th Ed. – Island Press, Washington, DC, pp. 49-68.

[5] Deng, X., Xu, Y., Han, L., Song, S., Yang, L., Li, G., Wang, Y. (2015): Impacts of urbanization on river systems in the Taihu Region, China. – Water 7: 1340-1358. https://doi.org/10.3390/w7041340.

[6] Han, J., Hu, Z., Wang, P., Yan, Z., Li, G., Zhang, Y., Zhou, T. (2022): Spatio-temporal evolution and optimization analysis of ecosystem service value—a case study of coal resource-based city group in Shandong, China. – Journal of Cleaner Production 363: 132602. https://doi.org/10.1016/j.jclepro.2022.132602.

[7] He, B., Feng, Y., Wu, W., Fan, W. (2010): Recent ten years spatiotemporal variation characteristics of vegetation index in Anhui Province. – Chinese Journal of Ecology 29(10): 1912-1918 (in Chinese).

[8] Hu, J., Zhang, J., Li, Y. (2022): Exploring the spatial and temporal driving mechanisms of landscape patterns on habitat quality in a city undergoing rapid urbanization based on


http://www.aloki.hu ● ISSN 1589 1623 (Print) ● ISSN 1785 0037 (Online)
DOI: http://dx.doi.org/10.15666/aeer/2305_91019120

GTWR and MGWR: the case of Nanjing, China. – Ecological Indicators 143: 109333. https://doi.org/10.1016/j.ecolind.2022.109333.

[9] Hu, Z., Xiao, W., Fu, Y. (2013): Introduction to concurrent mining and reclamation for coal mines in China. – Twenty Second International Symposium on Mine Planning Equipment Selection. October 14-19. Dresden/Freiberg, Germany pp. 781-789. https://doi.org/10.1007/978-3-319-02678-7_76.

[10] Li, Y., Chang, Y., Hu, Y., Li, X., Xiao, D. (2006): Research advance in effects of anthropogenic activity on forest landscape. – Scientia Silvae Sinicae 42(9): 119-126 (in Chinese).

[11] Li, Y., Wang, H., Wang, R., Zhang, Y., Song, M., Liu, J. (2020): Tradeoffs and time lag in ecosystem services during degradation and restoration processes in a freshwater lake region in northern China. – Polish Journal of Environmental Studies 29(2): 1219-1228. https://doi.org/10.15244/pjoes/106033.

[12] Li, Z., Chang, J., Li, C., Gu, S. (2023): Ecological restoration and protection of national land space in coal resource-based cities from the perspective of ecological security pattern: a case study in Huaibei City, China. – Land 12(2): 442. https://doi.org/10.3390/land12020442.

[13] Liu, D., Zhou, L. (2021): Effects of landscape pattern changes on bird diversity in AnqingCazi Lake National Wetland Park, Anhui,China. – Chinese Journal of Ecology 40(7): 2201-2212 (in Chinese).

[14] Liu, H., Zhu, X., Cheng, H., Su, L., Dai, L., Zheng, L., Fang, S., Jiang, C., Zhang, Q., Sun, Q., Li, Y., Li, D. (2021): Key technology of human environment and ecological reconstruction in high submersible level coal mining subsidence area: a case study from Lüjin Lake, Huaibei. – Journal of China Coal Society 46(12): 4021-4032 (in Chinese). https://doi.org/10.13225/j.cnki.jccs.2021.1499.

[15] Liu, Y. X., Wang, Y. L., Peng, J., Yuan, Y., Ma, J., Wei, H. (2015): Selection of different clustering algorithms for settlement landscape aggregation in suburb. – Scientia Geographica Sinica 35(6): 674-682. https://doi.org/ (in Chinese).

[16] Ma, Z., Duan, X., Wang, L., Kang, Y., Yun, R. (2023): A scenario simulation study on the impact of urban expansion on terrestrial carbon storage in the Yangtze River Delta, China. – Land 12(2): 297. https://doi.org/10.3390/land12020297.

[17] Qian, F. K., Pang, R. R., Yu, Y., Xu, H., Han, C. L. (2023): Spatial correlation characteristics and mechanism of cultivated land landscape pattern and cultivated land quality in different geomorphic areas of Liaoning Province. – Chinese Journal of Eco-Agriculture 31(1): 113−124 (in Chinese).

[18] Redo, D. J., Aide, T. M., Clark, M. L., Andrade-Núñez, M. J. (2012): Impacts of internal and external policies on land change in Uruguay, 2001-2009. – Environmental Conservation 39(2): 122-131. https://doi.org/10.1017/S0376892911000658.

[19] Roces-Díaz, J. V., Vayreda, J., Banqué-Casanovas, M., Díaz-Varela, E., Bonet, J. A., Brotons, L., de-Miguel, S., Herrando, S., Martínez-Vilalta, J. (2018): The spatial level of analysis affects the patterns of forest ecosystem services supply and their relationships. – Science of the Total Environment 626: 1270-1283. https://doi.org/10.1016/j.scitotenv.2018.01.150.

[20] Song, Y., Yeung, G., Zhu, D., Xu, Y., Zhang, L. (2022): Efficiency of urban land use in China's resource-based cities, 2002-2018. – Land Use Policy 115: 106009. https://doi.org/10.1016/j.landusepol.2022.106009.

[21] Sun, Y., Lu, M., Wang, Y., Yang, Z. (2022): Ecosystem health assessment of Fen River basin based on landscape pattern evolution. – China Rural Water and Hydropower 1-16 (in Chinese).

[22] Sutton, P. C., Costanza, R. (2002): Global estimates of market and non-market values derived from nighttime satellite imagery, land cover, and ecosystem service valuation. – Ecological Economics 41: 509-527. https://doi.org/10.1016/S0921-8009(02)00097-6.


http://www.aloki.hu ● ISSN 1589 1623 (Print) ● ISSN 1785 0037 (Online)
DOI: http://dx.doi.org/10.15666/aeer/2305_91019120

[23] The National Bureau of Statistics of the People's Republic of China (2022): Statistical Communique of the People's Republic of China on the 2021 National Economic and Social Development. – http://www.stats.gov.cn/tjsj/zxfb/202302/t20230227_1918980.html (in Chinese).
[24] United Nations (2001): System of Environmental and Economic Accounting. – SEEA 2000 Revision. United Nations, New York.
[25] Xiao, W., Fu, Y., Wang, T., Lv, X. (2018): Effects of land use transitions due to underground coal mining on ecosystem services in high groundwater table areas: a case study in the Yanzhou coalfield. – Land Use Policy 71: 213-221. https://doi.org/10.1016/j.landusepol.2017.11.059.
[26] Xie, G., Lu, C., Leng, Y. (2003): Ecological assets valuation of the Tibetan Plateau. – Journal of Natural Resources 18(2): 189-196 (in Chinese).
[27] Xie, G., Xiao, Y., Zhen, L., Lu, C. (2005): Study on ecosystem services value of food production in China. – Chinese Journal of Eco Agriculture 13(3): 10-13 (in Chinese).
[28] Xie, G., Zhen, L., Lu, C., Xiao, Y., Chen, C. (2008): Expert knowledge based valuation method of ecosystem services in China. – Journal of Natural Resources 23(5): 911-919 (in Chinese).
[29] Yan, Y., Li, J., Lu, X., Wang, Y., Li, M. (2023): Identifying an over tenfold variation in carbon intensities of coal mines in China by multi-scale multi-benchmark accounting. – Journal of Cleaner Production 384: 135621. https://doi.org/10.1016/j.jclepro.2022.135621.
[30] Yang, H., Cao, J., Hou, X. (2023): Study on the evaluation and assessment of ecosystem service spatial differentiation at different scales in mountainous areas around the Beijing-Tianjin-Hebei Region, China. – International Journal of Environmental Research and Public Health 20(2): 1639. https://doi.org/10.3390/ijerph20021639.
[31] Yu, Q., Feng, C., Shi, Y., Guo, L. (2021): Spatiotemporal interaction between ecosystem services and urbanization in China: incorporating the scarcity effects. – Journal of Cleaner Production 317: 128392. https://doi.org/10.1016/j.jclepro.2021.128392.
[32] Zhang, X., Ren, W., Peng, H. (2022): Urban land use change simulation and spatial responses of ecosystem service value under multiple scenarios: a case study of Wuhan, China. – Ecological Indicators 144: 109526. https://doi.org/10.1016/j.ecolind.2022.109526.
[33] Zhang, S., Wang, Y., Wang, Y., Li, Z., Hou, Y. (2023a): Spatiotemporal evolution and influencing mechanisms of ecosystem service value in the Tarim River Basin, Northwest China. – Remote Sensing 15(3): 591. https://doi.org/10.3390/rs15030591.
[34] Zhang, S., Wu, T., Guo, L., Zou, H., Shi, Y. (2023b): Integrating ecosystem services supply and demand on the Qinghai-Tibetan Plateau using scarcity value assessment. – Ecological Indicators 147: 109969. https://doi.org/10.1016/j.ecolind.2023.109969.
[35] Zhang, X., Shen, J., Sun, F., Wang, S. (2023c): Spatial-temporal evolution and influencing factors analysis of ecosystem services value: a case study in Sunan Canal basin of Jiangsu Province, Eastern China. – Remote Sensing 15(1): 112. https://doi.org/10.3390/rs15010112.
[36] Zhao, Y., Zheng, G., Bo, H., Wang, Y., Dong, J., Li, C., Wang, Y., Yan, S., Liu, K., Wang, Z., Liu, J. (2014): Habitats generated by the restoration of coal mining subsidence land differentially alter the content and composition of soil organic carbon. – PLoS ONE 18(2): e0282014. https://doi.org/10.1371/journal.pone.0282014.
[37] Zhou, Y. (2022): UDB demarcation and management and control of coal resource-based cities under EH (Master's thesis). – China University of Mining and Technology. 2022 (in Chinese).
[38] Zhou, Y., Chang, J., Feng, S. (2022): Effects of urban growth boundaries on urban spatial structural and ecological functional optimization in the Jining Metropolitan Area, China. – Land Use Policy 117: 106113. https://doi.org/10.1016/j.landusepol.2022.106113.


http://www.aloki.hu ● ISSN 1589 1623 (Print) ● ISSN 1785 0037 (Online)
DOI: http://dx.doi.org/10.15666/aeer/2305_91019120